



HAL
open science

CoboShell Robot for Automatic Scallop Shelling Process: Concepts and Applications

Othman Lakhall, Abdelkader Belarouci, Xinrui Yang, Taha Chettibi, Rochdi
Merzouki

► **To cite this version:**

Othman Lakhall, Abdelkader Belarouci, Xinrui Yang, Taha Chettibi, Rochdi Merzouki. CoboShell Robot for Automatic Scallop Shelling Process: Concepts and Applications. 2023 IEEE/ASME International Conference on Advanced Intelligent Mechatronics (AIM), Jun 2023, Seattle, France. pp.157-163, 10.1109/AIM46323.2023.10196232 . hal-04402881

HAL Id: hal-04402881

<https://hal.science/hal-04402881>

Submitted on 18 Jan 2024

HAL is a multi-disciplinary open access archive for the deposit and dissemination of scientific research documents, whether they are published or not. The documents may come from teaching and research institutions in France or abroad, or from public or private research centers.

L'archive ouverte pluridisciplinaire **HAL**, est destinée au dépôt et à la diffusion de documents scientifiques de niveau recherche, publiés ou non, émanant des établissements d'enseignement et de recherche français ou étrangers, des laboratoires publics ou privés.

CoboShell Robot for Automatic Scallop Shelling Process: Concepts and Applications

Othman Lakhal, Abdelkader Belarouci, Xinrui Yang , Taha Chettibi and Rochdi Merzouki

Abstract—Shelling scallops can be a labor-intensive and repetitive task that can lead to musculoskeletal disorders for the operators. The repetitive nature of the task and the force required to open the scallop shells can significantly strain the hands, wrists, and arms of the operators. In this study, we explored the automation of the shelling process in the seafood industry. We introduced a new mechatronic system called CoboShell, which automates the opening of scallops and the cutting of the nut muscle using a collaborative robot (cobot). CoboShell ensures the preservation of the quality of the fresh sea product. Initially, we addressed a technological challenge by proposing an integrated solution based on the Venturi effect. We used appropriately sized suction cups to handle the non-uniform surfaces of the shells. Subsequently, we focused on a scientific inquiry involving the control of the knife blade's trajectory using a cobot. The goal was to guide a flexible knife blade along the inner flat part of the scallop shell. This process aimed to cut the nut muscle and separate the two parts of the scallop. For that, the entry point of the knife is determined automatically in the centre of the scallop opening using an Artificial Intelligence (AI) based technique. Finally, experimental results as well as the repetitive tests have shown that the cobot provided better quality on the muscle cutting with high accuracy and cadence, comparing to conventional industrial arm in the automation of the scallop shelling process.

Index Terms—Automatic scallop shelling, Collaborative robot, Artificial intelligence, Force-compliance control.

I. INTRODUCTION

SCALLOPS are commercially important shellfish worldwide, with over 40 commercially exploited species of bivalve shellfish. These shellfish are frequently harvested or cultivated to meet the high demand [1]. Scallops are usually processed into frozen adductor muscles for sale and export. Manual shelling is the most reliable method for removing the meat from the shell while retaining its quality for raw consumption.

Bivalve molluscs like black scallops, scallops, and oysters have two shells or valves connected by a ligament along the hinge, held closed by an adductor muscle called a nut. When these molluscs are taken out of their natural environment, the adductor muscles contract, tightly linking the two valves together. Extracting the flesh from inside the shell requires separating the adductor muscles from the valve, traditionally done by inserting a knife. Manual shelling ensures the physical integrity, sensory quality, and sanitation of the meat, but it demands skilled individuals with strength and experience

[2]. Manual shelling is performed by inserting a knife blade near the hinge of the shells and carefully separating the nut without causing damage. This technique offers more control and precision compared to mechanical or automated methods, resulting in a superior quality product. The process of manual shelling follows the steps shown in Figure 1.

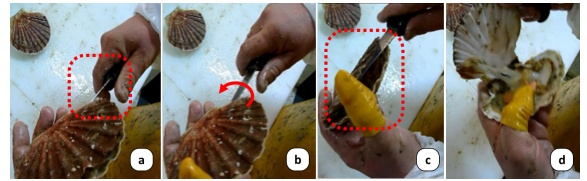


Fig. 1: Manual process of scallop shelling : (a) Holding the scallop with the hollow shell, inserting the knife into a small opening. (b) Leveraging the knife to lift the flat part and open the scallop. (c) Securing the flat part with the thumb and sliding the knife to cut the adductor muscle. (d) Breaking the hinge to separate the flat part from the hollow part of the scallop.

The quality of the nut recovered and the amount of adductor muscle remaining attached to the shell vary from person to person, posing challenges when dealing with a large number of shells. If not treated promptly, the freshness of the flesh decreases, particularly with manual shelling. Moreover, the manual shelling process often leads to wrist problems, microtraumas, and musculoskeletal disorders due to the required force to hold the shell open during muscle separation. The scallop shelling sector faces declining attractiveness in shelling activities and the need to enhance and ensure the quality of landed scallop products.

Addressing the problem of separating the shell from the mollusc meat, regardless of the processed products, is crucial. Automation or robotisation of scallop shelling is of particular interest in the food processing industry, as it can process large quantities of scallops in a short time. Various shelling methods have been developed to assist manual sheller, with a significant increase in inventions and innovations in this field. Martin [3] provides a review comparing the advantages and disadvantages of different scallop shelling technologies, including mechanical, thermal, and pressure-based processes.

Steam machines [4] and high-pressure (HP) shelling [5] have been proposed, but they can significantly alter the moisture, pH, color, and texture of the adductors. High hydrostatic pressure (HHP) has been explored as an alternative for scallop shelling [5], but it must be applied thoroughly to avoid scale appearance in the muscles. Heating and cooling processes

have also been used for scallop shelling [6], [7], but they compromise freshness by cooking the product.

Other methods, such as laser technology, have been applied to sever the adductor muscle precisely [8], but their use is limited to certain mollusc species. Numerous patents exist, reflecting the ongoing efforts to automate scallop shelling. Mechanical, cold, electric discharge, hot or steam, and high-pressure processes have been explored [9], [10], [11], [12], [13], [14]. However, these methods often result in mutilation or cooking of the nut, hindering the live recovery of scallops in good condition. Despite the progress made so far, there is still a need to develop an affordable and efficient shelling method that preserves quality and allows for the live recovery of scallops in good condition [15].

Developing an automatic scallop shelling device that minimises impurities and maintains product quality poses a significant challenge. Replicating the manual shelling process is crucial to preserve the raw consumption characteristics and production conditions. The device must separate the shell surfaces without breakage, minimise waste, and ensure the adductor muscle remains uncooked and alive. Additionally, the scallop fishing season is limited to a few months per year. The compact and easily installable CoboShell device presented in this article addresses these requirements and can be tailored to optimise the working area. Real-time control of the knife robot-guide's kinematics during the shell opening process is the scientific problem addressed. The paper's structure includes sections on the CoboShell system and shell opening detection methodology (Section II), modelling and control of the shelling system (Section III), experimental results and discussions (Section IV), and concluding remarks (Section V).

II. SYSTEM AND PROCESS DESCRIPTION

In this section, we will outline our concept for processing freshly caught scallops, obtaining shelled scallops while keeping the animal alive. Then, we will also provide a detailed description of the components of our scallop shelling system.

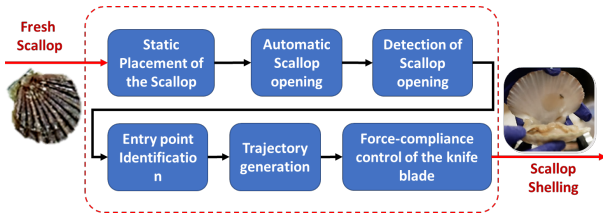


Fig. 2: System flowchart describing the process steps

The proposed process in this article is used to treat freshly caught shellfish, as shown in Fig. 2. The shells are placed manually or automatically by another system on a conveyor in a vertical position on a support. After fixing the shell holder with stops installed on the conveyor, the system opens the shells by separating the two valves held by the muscle. This separation, known as opening, is detected by a vision system based on a learning algorithm. The latter, by image processing, locates and returns the coordinates of the entry point of the knife tip. Finally, the system cuts the muscle to

recover the curved shell containing the live animal. This will then be processed by an operator or another system. The table I shows the dimensions of the scallops during the different fishing seasons. This information was used to design a specific support by rapid prototyping, capable of adapting to different sizes of scallops shells and keeping them in vertical positions.

TABLE I
Dimensions of scallop shells

Length [mm]		Width [mm]		Depth [mm]		Weight [g]	
Min	Max	Min	Max	Min	Max	Min	Max
110	140	110	140	20	30	130	240

The system comprises a scallop opening system, a camera for detecting the opening and locating the insertion point, and a knife guided by a cobot for muscle cutting, as depicted in Figure 3. Unlike mechanical methods, the proposed system is designed to minimise contact with the live animal and reduce the risk of shell breakage. This ensures that the bivalve mollusc remains alive and uncooked throughout the process, resulting in shelling with minimal impurities and without compromising product quality.

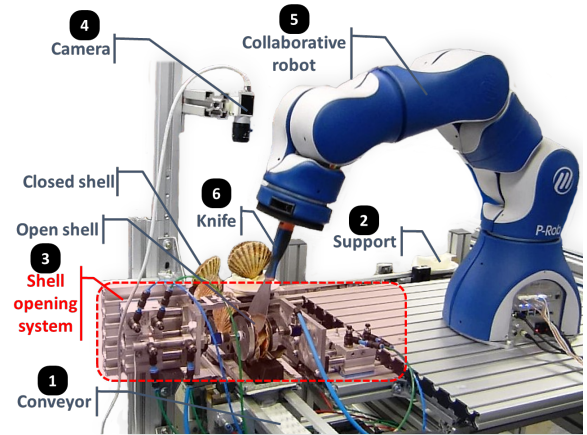


Fig. 3: CoboShell description : The shell is on a conveyor (1) in a vertical position on a support (2), the opening system (3) applies compliance to different types of valve surfaces using a vacuum system. The detection of the opening and the location of the entry point of the knife tip is achieved by a vision system (4). Finally, the adductor muscle is cut using a cobot (5) that guides the knife blade (6) along the flat shell for minimal material loss.

A. Shell opening system

The opening system consists of two rigid suction cups adapted to optimise contact with the shell whether it is rough or smooth, dirty or clean, flat or domed, so as to obtain a good airtight seal. Indeed, the shape of the scallop shell is jagged and not regular. In addition, the valves are ridged and are not symmetrical: one side is flat and the other curved. Thus, a small suction cup is used for the curved part, and a large suction cup for the flat part, which guarantees optimal contact regardless of the size of the shell, as shown in Fig. 4. In order to allow a good softness of the suction pads,

an universal joint has been added linking the suction cup to the cylinder. During the opening procedure, it is essential to adapt the orientation of the suction cup to the inclination of the valves. Three pneumatic cylinders are used to grip and

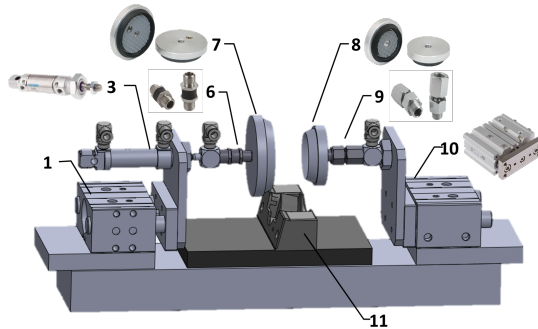


Fig. 4: Description of the automatic scallop opening mechanism : (1) and (10) Guided pneumatic cylinder. (3) Pneumatic cylinder. (6) Flexible suction cup mounted on curved surfaces. (7) and (8) Flexible suction cup mounted on flat surfaces. (9) Free-control joint to facilitate the suction cup compliance to curved surfaces. (11) Scallop shell support.

open the shells. These actuators are operated simultaneously to secure the shell without causing any impact. One specific actuator (3) is activated to achieve a partial opening of at least 10 mm in the flat valve, allowing the knife to pass between the valves and slide along the flat valve for muscle cutting. After the muscle is cut, the guided cylinder (1) is engaged to break the hinge and remove the flat valve. The vacuum is then released from the suction cups to separate the shell parts. The guided cylinder (10) is retracted to its initial position, enabling the operator to retrieve the assembly. An air-jet pump generates the vacuum, and vacuum sensors ensure a vacuum level between 60 and 70%. Positioning the vacuum sensor and air-jet pump close to the suction cup is crucial for optimal operation and maximum vacuum efficiency. The recommended maximum distances are 200 mm for the air-jet pump and 100 mm for the sensor based on testing. Due to the external force (ambient air) being greater than the internal force, the suction cup and the part remain connected throughout the procedure. It is important to note that opening a freshly caught shell may require a significant force approximately 70 N.

B. Detection and location of opening

A deep learning-based approach has been implemented for the detection and localization of shell opening area, as reported in [16]. The approach uses images captured by a visual sensor (camera) located above the opening system to detect the opening area of the shell, as illustrated in Fig. 5-a. The model's output provides a binary mask that covers the opening area between the two walls of the shell, as shown in Fig. 6. From this binary mask, the contour of the opening is determined by calculating the central moment of the binary mask, as shown in Fig. 5-b. Furthermore, by applying the morphological transformation of the median axis, a central line (i.e., a skeleton) can be extracted from the opening area. The entry point is then calculated by determining the central point

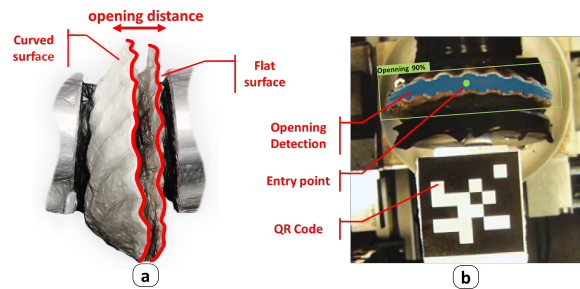


Fig. 5: (a) Considered scallop parts for the deep learning (b) Segmentation model for automatic detection of scallop opening.

of the central line of the opening area. The location of the entry point in the industrial arm frame is subsequently determined by applying a transformation. To achieve this, a QR Code is placed in the image frame for precise localization (Fig. 5-b). The instance segmentation model that we choose is Mask RCNN [17], it has been implemented in other single-target-single-class instance segmentation tasks in multiple fields and has shown better performance compared to other models in term of efficiency and precision. The model is constructed with a backbone consisting of a ResNet50 and a Feature Pyramid Network (FPN), as shown in Fig. 6. A shell-opening

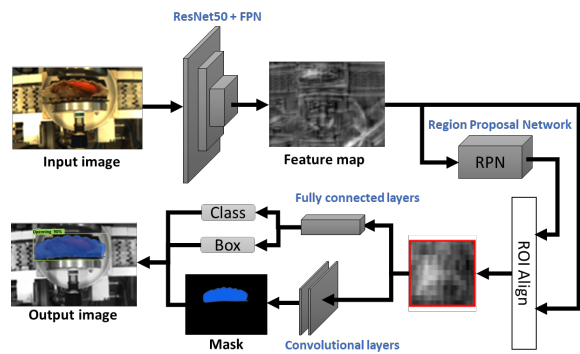


Fig. 6: Architecture of Mask RCNN for automatic detection of the scallop opening.

image dataset is collected for the training of the model. The dataset is divided into a training set containing 130 images and a validation set containing 34 images. All the images are taken from top-view, each image contains a closed or open shell with different size of opening and different background set up. To enhance the generalization and robustness of the instance segmentation model, data augmentation techniques were applied online during the training process. The considered augmentations included random flipping, as well as random adjustments to contrast and brightness to simulate various lighting conditions and enrich the diversity of the dataset. The model's performance can be improved in handling a wider range of scenarios. By using a transfer learning approach, a pre-trained model was fine tuned on the custom dataset on a DELL workstation with Intel® Core™ i9-11950H CPU and NVIDIA RTX A3000 GPU. The model's performance was evaluated on the validation dataset by using

the mean average precision (mAP) metric which considers the segmentation quality of the model predictions. The mAP score was calculated over multiple Intersection over Union (IoU) thresholds ranging from 0.5 to 0.95 with a step of 0.05 and achieved a mAP score of 75.7%.

C. Collaborative Robot (cobot)

The cobot is utilized to guide the knife blade such that it passes between the two shells and cuts the muscle, after the opening. The specific robot used is the P-Rob 2R developed by F&P Robotics AG. This robot is lightweight and its computer is integrated within the structure, simplifying the installation and manual movement. The P-Rob 2 robotic arm is a 6 degree of freedom (DoF) manipulator.

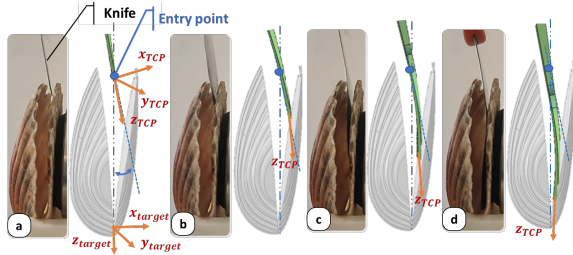


Fig. 7: Tool Centre Point (TCP) of the Knife blade's trajectory under compliance interaction

Additionally, it is force-limited and detects collisions, preventing damage to the shell in the event of impact in our context. This is because the blade of the knife must be in contact with the flat surface of the shell throughout the cutting of the muscle. In addition, it is important to note that the shelling trajectory varies according to the size of the shell and the opening distance. The effort required to open each shell is different. Although the opening cylinder's range is limited to 2 cm, it rarely reaches this limit with freshly caught shells. In order to insert a knife and cut the muscle, the opening distance must be greater than 10 mm. The vision system described in the previous section returns the coordinates of the entry point. The cobot must guide the knife blade towards the entry point. Once the entry point is reached by the blade, it becomes a constraint on the robot's kinematics. As illustrated in the Fig. 7, the orientation of the knife must be relative to the entry point while maintaining contact with the flat surface to prevent material loss, by adjusting the compliance accordingly.

III. MODELLING AND CONTROL OF THE SYSTEM

In this section, we describe the steps for the trajectory control of the knife blade tip based on the cobot.

A. kinematics transformation

Let's affect the frame \mathcal{R}_0 to the base of the cobot, the frame \mathcal{R}_{TCP} to the knife blade tip, the frame \mathcal{R}_{QR} to the center of the QR Code, the frame \mathcal{R}_C to the camera and the frame \mathcal{R}_{SO} to the scallop opening mechanism, as presented in the Fig. 8. ${}^0_{TCP}T$ is the transformation of the knife blade tip with respect to the basis frame of the cobot. This transformation is obtained

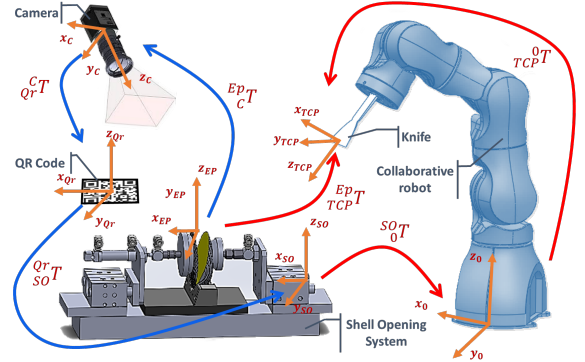


Fig. 8: Kinematic frames of cobot and vision systems

from the Forward Kinematic Model (FKM) based on the joint positions. Transformation ${}^0_{SO}T$ between the cobot frame and that of the scallop opening mechanism is measured during the preparation stage. The TCP has been calibrated according to the cobot frame. The QR Code is attached to the frame of the scallop opening mechanism, so the transformation ${}^{QR}_{SO}T$. Through a vision system based on a camera, the transformation ${}^C_{QR}T$ of the QR Code position is detected. This method uses image analysis to identify the contours of the QR Code and determine its position. Finally, ${}^{EP}_{TCP}T$ is obtained from the RCNN mask described in the previous section. Thus, the entry point (EP) is calculated in the knife blade frame, which is the target point for introducing the knife into the scallop. The total kinematics transformation ${}^{EP}_{TCP}T$ is calculated using Eq. (1).

$${}^{EP}_{TCP}T = \underbrace{{}^{EP}_{C}T}{}^C_{QR}T \underbrace{{}^{QR}_{SO}T}{}^{QR}_{SO}T \underbrace{{}^{SO}_0T}{}^{SO}_0T \underbrace{{}^0_{TCP}T}{}^0_{TCP}T \quad (1)$$

Deep-Learning Cst Record FKM

B. CoboShell cobot Kinematics

Fig.9 represent the kinematics chain of the 6-DoF Cobot. The forward kinematic equations are obtained from the modified Denavit-Hartenberg (D-H) parameters, which describes the homogeneous transformation matrix ${}^{i-1}T_i$, where i is the joint number. Finally, the position of the tool frame with respect to the cobot frame is obtained as follows:

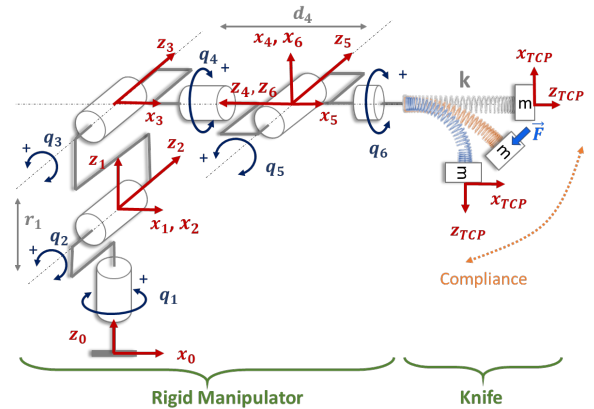


Fig. 9: CoboShell cobot kinematics chain.

$${}^0_{TCP}T = {}^0_1T {}^1_2T {}^2_3T {}^3_4T {}^4_5T {}^5_6T {}^6_{TCP}T \quad (2)$$

${}^0_{TCP}T$ represents the position and orientation of knife blade tip as a function of the six joint variables q_i where $i = [1..6]$. ${}^6_{TCP}T$ describes the transformation between the end joint frame and the knife blade TCP frame. This changes based on the type of compliance exhibited by the blade and can be estimated by measuring the applied force obtained from the cobot. The Inverse Kinematic Model (IKM) calculates the joint variables θ_i based on the pose (position and orientation) of the knife tip. Paul's method [18], a technique for solving the inverse kinematic problem in robots with simple geometry, as seen in previous works [19]. The IKM is also utilised for trajectory planning, as reaching a specific target point can be achieved in various ways depending on the knife's orientation. The kinematic model is essential for controlling the knife tip and verifying the knife tip's accessibility based on constraints.

Let EP a entry point be defined by ${}^0_{EP}T$ expressed in frame \mathcal{R}_0 of the robot as shown in Fig. 8. As previously mentioned in previous sections, the target point varies from one shell to another. It is dependent on both the size of the shell and the opening distance. For this purpose, we assume that the opening forms an isosceles triangle as shown in Fig. 10, with a the opening distance obtained by the vision system and h the height which is the distance from the entry point to the shell hinge, can be considered constant as it depends on the fishing season for which the size is knowledge.

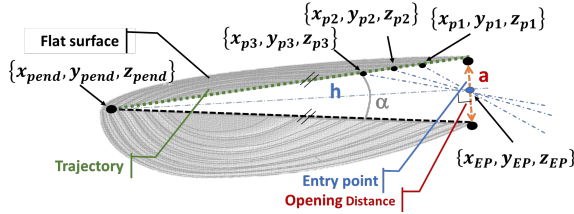


Fig. 10: Assumption: the opening of the shell forms an isosceles triangle

Thus from the opening distance and the height, the opening angle α can be calculated and the trajectory of the knife tip can be deduced. Based on the coordinates of the entry point $\{x_{EP}, y_{EP}, z_{EP}\}$ and the trajectory points $\{x_{pi}, y_{pi}, z_{pi}\}$, with i the number of the point, the vector \mathbf{w} of the matrix ${}^0_{EP}T$ can be obtained as follows:

$$\mathbf{w} = \frac{[x_{pi} - x_{EP}, y_{pi} - y_{EP}, z_{pi} - z_{EP}]^T}{\sqrt{(x_{pi} - x_{EP})^2 + (y_{pi} - y_{EP})^2 + (z_{pi} - z_{EP})^2}} \quad (3)$$

The vector \mathbf{u} is normal to the vector \mathbf{w} and is parallel to the plane ZX

$$\mathbf{u} = \frac{[w(3), 0, -w(1)]^T}{\sqrt{(w(3))^2 + (-w(1))^2}} \quad (4)$$

The vector \mathbf{v} is perpendicular to the plane formed by the vectors \mathbf{u} and \mathbf{w}

$$\mathbf{v} = \mathbf{w} \wedge \mathbf{u} \quad (5)$$

Thus, the rotation matrix of ${}^0_{EP}T$ can therefore be deduced for each target point.

IV. EXPERIMENTAL RESULTS

The current average rate of manual scallop shelling is 5 shells/minute/person. It should be noted that the tests were carried out under real conditions in humid environment and a temperature of between 2 and 8°C. In this study, among the 67 shells that were shelled on the day of fishing, 5 shells could not be opened by the system due to their surface degrading during fishing. Indeed, the vacuum could not be made correctly. Moreover, tests on about thirty shells made it possible to determine the effort required to open a fresh shell, the force required being between 40 and 70 N. With an opening rate of over 90%, this proves the robustness of our system, especially on freshly caught shellfish while preserving their quality. Vacuum adsorption is a technique widely used in many robotic fields. The size of the suction cups depends on the type of contact surfaces and the applied efforts for the grasping [20] or the loading hold. The main difficulty for the scallop surface is its irregularities, where even if the soft material of the suction cups, such as thin-film polymer, poly (3, 4-ethylenedioxythiophene) [21] allows a perfect compliance to the surface of the scallop, it generates the air leaks due to the contact with the surface irregularities under air pressure equivalent to 70N of effort, compared to regular surfaces of fruits as an example. Several types and sizes of suction cups were tested to obtain the type of suction cup that would have a perfect grip by adapting to irregular surfaces. In the end, flat and round suction cups with an aluminium support plate were chosen, as shown in the Fig. 11. This vacuum has been adapted by removing the internal part in order to optimise contact with the scallop shell and better manage depression whether rough or smooth, dirty or clean, flat or convex.

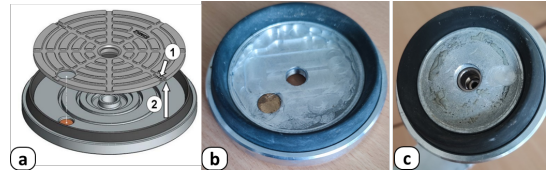


Fig. 11: Description of the modified suction cup : (a) Removing the rubber disc from the existing suction cup. (b) Large suction cup for the flat part (80 mm) (c) Small suction cup for the curved part (55 mm).

Fig. 12 illustrates the knife trajectories for a set of shells from different views. The generation of the knife trajectory is observed to adapt to the shell size but also to the opening distance through the insertion point. The measured trajectory is obtained by FKM from the coordinates of the joints. The trajectory performed by the robot is smoothed using a smoothing parameter in the robot language. We observe that the knife deviates +/- 5mm from its desired trajectory. However, this is not a problem because the blade of the knife is flexible, on the contrary, it favours the cutting of the muscle. Fig. 12 also shows the accuracy of our detection and localisation based on deep learning. As the robot is a cobot, the speed of its joints is limited to between 50 and 100 deg/s. The peeling rate obtained is about 5 seconds/shell. Other tests were carried out with an industrial robot and we were able to reach 2 seconds/shell.

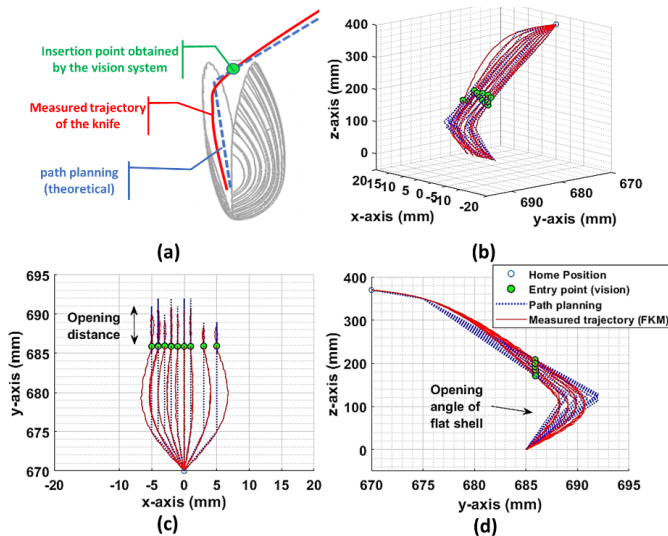


Fig. 12: Trajectories of knife tip performed for the shelling of 15 scallops : (a) Parameters representation (b) 3D view. (c) top view. (d) view on the zy plane.

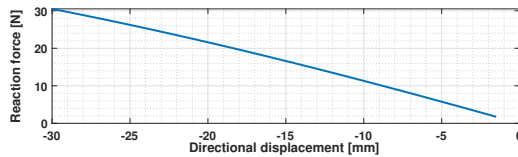


Fig. 13: Deformation of the knife as a function of the reaction force.

Fig 13 describes the laboratory tests conducted on the knife blade bending. They allow obtaining the linear characteristic of the stiffness based on the relation between the external effort and the bending displacement. Finally, the laboratory tests allows to identify the stiffness of the knife blade and establish the desired force profile to ensure a stable compliance during the cutting task. This enables more effective and optimal contact with the scallop, thereby enhancing the quality of the shelling process. In summary, this approach represents a noteworthy improvement over existing scallop shelling methods employed in the industry.

V. CONCLUSION

This article deals with a new integrated concept of automatic scallop shelling, called CoboShell. The latter consists of a system for the automatic opening of the scallop shells by the venturi effect, caused by two compliant suction cups, sized in relation to the profiled surface on each side of the scallop shell. A vision system was coupled with artificial intelligence tools for deep learning to accurately determine the shape and width of the opening as well as the position of the entry point to reach the nut muscle. A collaborative robot (cobot) was used to guide the knife blade on a curvilinear trajectory that could reach the scallop muscle. The cobot is controlled in force and compliance to manage interaction with the flat shell surface, following a parametric curve. CoboShell has been designed to replicate the manual shelling process and maintain

the quality of the fresh sea product. Experimental results show conformance control performance with 90% material removed and a rate of approximately 5 seconds/scallop.

ACKNOWLEDGMENT

This work was funded by the Regional Funds for Research and Innovation Hauts-de-France (2015-2020) under the name COBOFISH with the reference: DRESS-2018-006407 and the regional network S-MART Hauts-de-France.

REFERENCES

- [1] W. D. DuPaul, R. A. Fisher, and J. E. Kirkley, "An evaluation of at-sea handling practices: Effects on sea scallop meat quality, volume and integrity," 1990.
- [2] C. Lu, C. Cai, J. Zhang, A. Wang, and F. Li, "Application of response surface methodology in scallop shelling," 2021.
- [3] D. E. Martin and S. G. Hall, "Oyster shucking technologies: past and present," *International journal of food science & technology*, vol. 41, no. 3, pp. 223–232, 2006.
- [4] J. Zhang, J. G. Yi, H. Y. Jiang, J. Z. Wang, and J. T. Liu, "Research on control system of steam scallop shelling machine," in *Applied Mechanics and Materials*, vol. 441. Trans Tech Publ, 2014, pp. 879–882.
- [5] J. Yi, Q. Xu, X. Hu, P. Dong, X. Liao, and Y. Zhang, "Shucking of bay scallop (*Argopecten irradians*) using high hydrostatic pressure and its effect on microbiological and physical quality of adductor muscle," *Innovative Food Science & Emerging Technologies*, vol. 18, pp. 57–64, 2013.
- [6] D. E. Martin, J. Supan, J. Theriot, and S. G. Hall, "Development and testing of a heat-cool methodology to automate oyster shucking," *Aquacultural engineering*, vol. 37, no. 1, pp. 53–60, 2007.
- [7] D. E. Martin, J. Supan, U. Nadimpalli, and S. G. Hall, "Effectiveness of a heat/cool technique for shucking oysters," *Aquacultural engineering*, vol. 37, no. 1, pp. 61–66, 2007.
- [8] G. Singh, "Laser modernizes oyster shucking," *Food technology*, 1972.
- [9] E. F. Kiczek, "Method for opening a mollusk," Feb. 12 1991, uS Patent 4,992,289.
- [10] F. Hanks Jr and W. C. Grieb Jr, "Method and apparatus for removing meat from the shells of bivalve mollusks," Jul. 27 1971, uS Patent 3,594,859.
- [11] C. T. Brown, "Apparatus for removing scallops from their shells," May 23 1967, uS Patent 3,320,631.
- [12] M. Yoshida, A. Sato, and N. Hukuoka, "Method and apparatus for peeling-off bivalve, as well as bivalve before-separation heating device," Jul. 11 2000, uS Patent 6,086,468.
- [13] W. K. Rodman and P. d. S. D. Prevost, "Method of shucking scallops and an apparatus therefor," Dec. 7 1982, uS Patent 4,361,933.
- [14] D. C. Earnshaw, "Shellfish processing apparatus," Nov. 11 1996, uS Patent 6,110,032.
- [15] D. E. Martin, *Optimization and automation of a thermal oyster shucking process*. Louisiana State University and Agricultural & Mechanical College, 2003.
- [16] X. Yang, M. Kahouadji, O. Lakhali, and R. Merzouki, "Integrated design of an aerial soft-continuum manipulator for predictive maintenance," *Frontiers in Robotics and AI*, vol. 9, p. 980800, 2022.
- [17] K. He, G. Gkioxari, P. Dollár, and R. Girshick, "Mask r-cnn," in *Proceedings of the IEEE international conference on computer vision*, 2017, pp. 2961–2969.
- [18] R. Paul, "Robot manipulators: mathematics, programming, and control, 1981," *equation*, vol. 1, p. 30, 1981.
- [19] O. Lakhali, A. Melingui, and R. Merzouki, "Hybrid approach for modeling and solving of kinematics of a compact bionic handling assistant manipulator," *IEEE/ASME Transactions on Mechatronics*, vol. 21, no. 3, pp. 1326–1335, 2016.
- [20] H. Zhu, Y. Guan, W. Wu, L. Zhang, X. Zhou, and H. Zhang, "Autonomous pose detection and alignment of suction modules of a biped wall-climbing robot," *IEEE/ASME Transactions on Mechatronics*, vol. 20, no. 2, pp. 653–662, 2015.
- [21] S. Aoyagi, M. Suzuki, T. Morita, T. Takahashi, and H. Takise, "Bellows suction cup equipped with force sensing ability by direct coating thin-film resistor for vacuum type robotic hand," *IEEE/ASME Transactions on Mechatronics*, vol. 25, no. 5, pp. 2501–2512, 2020.